Tribol Lett (2010) 40:155–165
DOI 10.1007/s11249-010-9651-z

ORIGINAL PAPER

The Effect of Morphology on the Tribological Properties of MoS_2 in Liquid Paraffin

Kun Hong Hu · Xian Guo Hu · Yu Fu Xu · Fei Huang · Jun Sheng Liu

Received: 28 April 2010 / Accepted: 22 June 2010 / Published online: 18 July 2010

Abstract The tribological properties of liquid paraffin (LP) containing molybdenum disulfide (MoS_2) additives, including nano-balls, nano-slices, and bulk 2H-MoS_2, are evaluated using a four-ball tribometer. Results show that all MoS_2 additives used can improve the tribological properties of LP, and that nanosized MoS_2 particles function as lubrication additives in LP better than micro-MoS_2 particles do. The LP with nano-balls presents the best antifriction and antiwear properties at the MoS_2 content of 1.5 wt%. This is ascribed to the chemical stability of the layer-closed spherical structure of nano-balls. The Stribeck curves confirm that the rotation speed of 1,450 rpm used is located at the mixed lubrication region under 300 N. MoS_2 nano-slices have small sizes and easily enter into the interface of the friction pair with a roughness of 0.032 μm, functioning as a lubricant in LP better than nano-balls do at the MoS_2 content of 1.0 wt%. The Stribeck curves also show that the differences between the two nano samples were magnified at high rotation speeds in hydrodynamic lubrication region. The application of nano-slices in high sliding speeds will be more advantageous. This work furthers the understanding of the relationship between the tribological properties and morphology of MoS_2.

Keywords Molybdenum disulfide · XPS · Solid lubricant additives

K. H. Hu (✉) · F. Huang · J. S. Liu
Department of Chemical and Materials Engineering, Hefei University, Hefei 230022, China
e-mail: hukunhong@163.com; hukunhong@gmail.com

X. G. Hu · Y. F. Xu
Institute of Tribology, Hefei University of Technology, Hefei 230009, China

1 Introduction

Molybdenum disulfide (MoS_2) is widely applied in solid lubrication and additives of lubricating oils and greases. The importance of MoS_2 as a lubricant lies in its relatively low friction coefficient and its chemical stability under high temperatures and vacuums. MoS_2 has a typical layered structure composed of strong S–Mo–S covalent bonds inside layers and weak Van der Waals gaps between layers. Easy sliding and weak Van der Waals gap between MoS_2 layers are generally regarded as significant features for its excellent lubricity.

Nanosized MoS_2 (nano-MoS_2) usually has better tribological properties, either in friction reduction or wear resistance, than bulk microsized MoS_2 (micro-MoS_2) [1–3]. Thus, nano-MoS_2 has attracted considerable attention, and some chemical routes to synthesize nanosized MoS_2 has been reported, including hydrothermal and solvothermal synthesis [4–6], decomposition of precursors [7, 8], surfactant-assisted synthesis [9], vapor phase deposition [10], and inverse micelle method [11]. Usable MoS_2 includes layer-closed MoS_2, such as inorganic fullerene-like nanoparticles and nano-tubes [12–18], as well as layer-opened MoS_2, such as bulk micro-MoS_2 and slice-like nano-MoS_2.

In previous articles, a quick precipitation method was designed to prepare molybdenum trisulfide (MoS_3) precursors in different shapes from sodium molybdate and sulfides [19, 20]. Heating the precursors could conveniently produce a hollow ball-like or slice-like nano-MoS_2 at 780 °C in H_2. In one study, lubrication properties of the as-prepared nano-MoS_2 in polyoxymethylene (POM) were investigated [21]. Results showed that layer-closed MoS_2 nano-balls without rim-edge surfaces were proper fillers in POM. However, layer-opened MoS_2 nano-slices, which feature a high BET area and active dangling bonds, have a degradation effect on the POM polymer [22].

MoS_2 nano-slices can degrade POM into poisonous formaldehyde during the thermal process; thus, it is difficult to add nano-slices to POM plastic. This implies that MoS_2 nano-slices are not proper for use in modifying POM plastic. Differences between the tribological properties of layer-closed MoS_2 nano-balls and the layer-opened nano-slices cannot, therefore, be fairly compared in the POM matrix. The present work investigates the tribological properties of MoS_2 samples, including nano-balls, nano-slices, and bulk MoS_2, in liquid paraffin. Liquid paraffin has a stable structure, and the addition of MoS_2 into the base oil need not be done at high temperatures. Thus, a just and comprehensive comparison between the two nano-MoS_2 samples may be obtained.

2 Experimental Section

2.1 Materials

Commercial bulk 2H-MoS_2 (micro-MoS_2, 325 mesh) was provided by Anhui Institute of Metallurgy, China. $Na_2MoO_4{\cdot}2H_2O$, $Na_2S{\cdot}9H_2O$, thioacetamide (TAA), hydrochloric acid (HCl), ethanol, liquid paraffin (LP), and other reagents used were of analytical grade.

2.2 Synthesis of Nano-MoS_2

2.2.1 Nano-balls

Ball-like MoS_3 precursors were synthesized by a quick homogenous precipitation method. The reaction solution was obtained by dissolving 2.5 mmol $Na_2MoO_4{\cdot}2H_2O$ and 15 mmol TAA in 100 mL distilled water. 10 mL Ethanol and 12 M hydrochloric acid (HCl) were subsequently added to the reaction system at 82 °C under fast stirring. The resulting precipitation was heated for 50 min at 780 °C in a high-purity (99.999%) H_2 atmosphere. The desired MoS_2 nano-balls, with an average diameter of 150 nm, were obtained. A more detailed demonstration for the preparation of MoS_2 nano-balls can be found in Ref. [20].

2.2.2 Nano-slices

Noncrystalline MoS_3 precursors were synthesized by a quick precipitation method. The reaction solution was obtained by dissolving 2.5 mmol $Na_2MoO_4{\cdot}2H_2O$, 15 mmol $Na_2S{\cdot}9H_2O$, and 10 mL ethanol in 100 mL distilled water at room temperature ($\sim$30 °C). Next, 12 M HCl was added to the reaction system under fast stirring. The resulting precipitation was heated for 50 min at 780 °C in a high-purity (99.999%) H_2 atmosphere. The desired MoS_2 nano-slices were obtained. A more detailed demonstration concerning the preparation process of MoS_2 nano-slices can be found in Ref. [19].

2.3 Characterization of MoS_2 Nanoparticles

MoS_2 nanoparticles were characterized using a FEI model Sirion 200 scanning electron microscope (SEM), a Hitachi model H-800 transmission electron microscopy (TEM), and a JEOL model JEM-2010 high-resolution transmission electron microscopy (HRTEM).

2.4 Tribological Tests

2.4.1 Samples

The kinetic viscosity of liquid paraffin (η) was tested according to the national standard of China (GB 10247-1988). Three kinds of MoS_2, namely, micro-MoS_2, MoS_2 nano-balls, and MoS_2 nano-slices, were each selected as lubrication additives in liquid paraffin (LP). The LP/MoS_2 samples, including 0, 0.5, 1.0, 1.5, and 2.0 wt% MoS_2 were obtained using ultrasonic dispersion for 10 min.

2.4.2 Tribological tests

Every LP/MoS_2 sample was again distributed using ultrasonic scattering for 5 min before tribological testing. The tribological behaviors of the obtained samples were investigated on an MQ-800 four-ball tribometer at 5 °C. The tests of friction reduction and wear resistance were conducted at a rotating speed of 1,450 rpm and a constant load of 300 N, which was selected according to the extra pressure value (P_B value) of LP (470 N, measured at 1,450 rpm for 10 s according to the ASTM D2783 standard). The steel balls (diameter 12.7 mm) used were fabricated according to the national standard of China (G20, GB/T308-2002 of China, Surface roughness $R_a = 0.032$ μm) from a quenched-and-tempered ASTM E52100 bearing steel with a hardness of 61–63 HRC. Wear rate was decided by the average wear scar diameter (WSD) ($\pm$0.01 mm) of the three bottom balls. The average wear scar diameters of the three bottom balls were measured using an optical microscope. Every test was repeated thrice, and their averaged values were used to evaluate the wear properties. The obtained wear scars were characterized using a VG model Escalab 250 X-ray photoelectron spectroscopy (XPS) and an optical microscope. The detailed testing process is demonstrated in Fig. 1.

3 Results and Discussion

3.1 Characterization of MoS_2 Nanoparticles

Figure 2 provides SEM micrographs of the obtained powders of MoS_2 nano-slices and nano-balls. The powders (Fig. 2a) consisted of a lot of agglomerated MoS_2

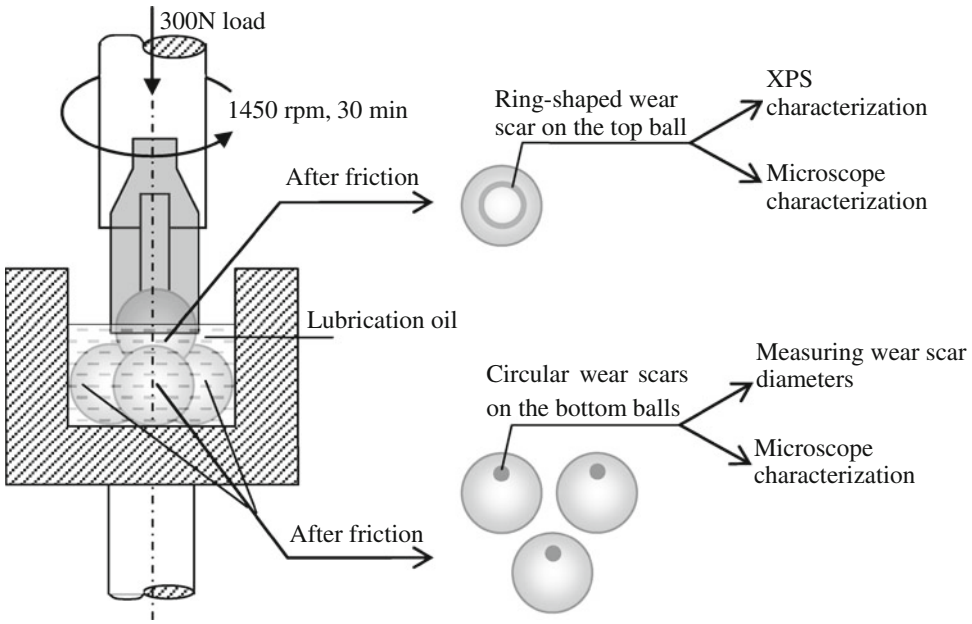

Fig. 1 Schematic of the four-ball tribological test

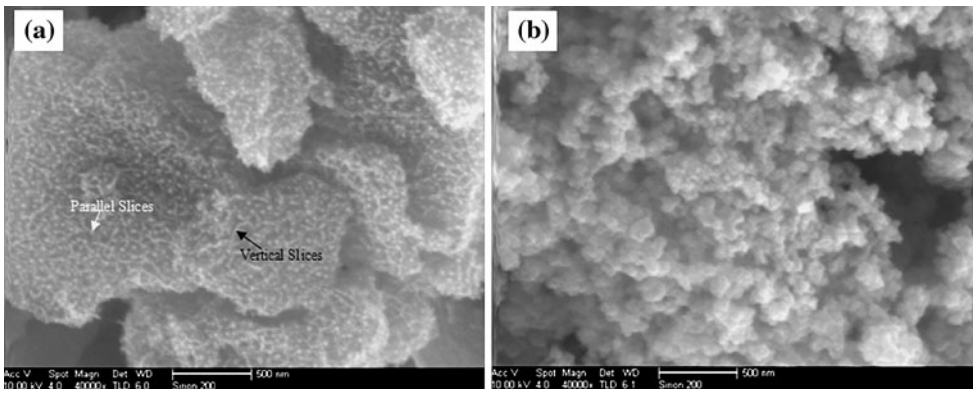

Fig. 2 SEM micrographs of MoS_2: **a** nano-slices and **b** nano-balls

nano-slices formed by the desulphurization of bulk MoS_3 [19]. However, the powder (Fig. 2b) was composed of agglomerated nano-balls. The structures of MoS_2 could not be clearly observed by SEM micrographs. Thus, the TEM and HRTEM characterization were done after ultrasonic dispersion in alcohol (Fig. 3).

The HRTEM micrographs of the obtained MoS_2 slices are provided in Fig. 3a. According to the micrograph in Fig. 3a, MoS_2 slices occurred in two manners on the copper net used in the HRTEM characterization: parallel or vertical to the copper net. The layered structure of MoS_2 was observed in the nano-slices vertical to the copper net. However, the nano-slices parallel to the copper net presented no layered structures, which hided on the side face. The thickness of the nano-slices varied from 5 to 10 nm, while their lengths from 10 to 40 nm. The distance between the two adjacent layers was about 0.625 nm.

Figure 4 shows the TEM and HRTEM micrographs of the obtained MoS_2 nano-balls. According to the micrograph shown in Fig. 4a, MoS_2 nano-balls has an average diameter of 150 nm. The HRTEM micrograph of the shell of a nano-ball confirms that the shell has a thickness of $\sim$11 nm containing 17 layers of MoS_2. The layer distance is about 0.64 nm, which is larger than that of the nano-slices.

3.2 Results of Tribological Tests

Figure 5a provides the variation of average friction coefficient with increasing MoS_2 content in LP at 1,450 rpm and 300 N. The LP sample with MoS_2 nanoparticles (nano-MoS_2), including nano-balls and nano-slices, presented better friction reduction properties than those with micro-MoS_2. When the nano-MoS_2 content was less than 1.5 wt% for nano-balls and 1.0 wt% for nano-slices, the average frictional coefficient of the LP/nano-MoS_2 system decreased with increasing nano-MoS_2 content within 30 min. Higher nano-MoS_2 content led to an increase in the average friction coefficient. These results indicate that the proper content of

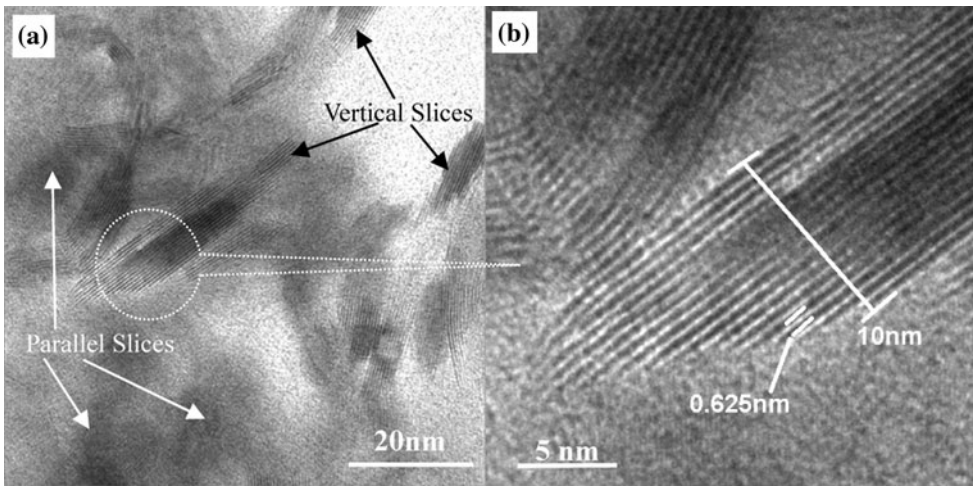

Fig. 3 HRTEM micrographs of MoS_2 nanoslices: **a** HRTEM micrograph and **b** the magnified part of **a**

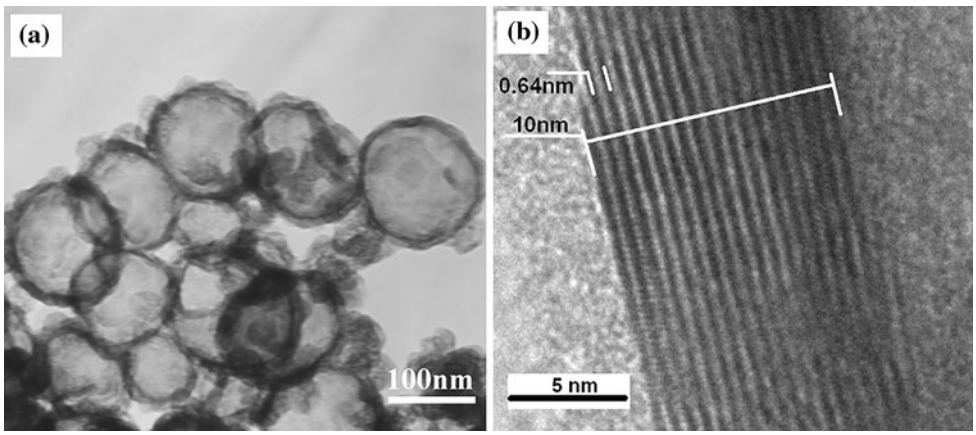

Fig. 4 TEM micrographs of MoS_2 nano-balls: **a** TEM and **b** HRTEM of shell of nano-balls

MoS_2 nano-balls in LP is 1.5 wt% while that of MoS_2 nano-slices in the same medium is 1.0%. The lowest friction coefficient occurs in the sample with 1.5% MoS_2 nano-balls.

The LP samples with 1.5 and 1.0% MoS_2 were then selected as testing samples for the friction-time curves under 300 N and 1,450 rpm, the results of which are provided in Fig. 5b. As shown in the figure, all friction coefficients increased with prolonged friction time. The prolonged friction time led to large WSDs and large contact areas between the top ball and the bottom balls, thus increasing the shearing and friction forces between the steel balls. As such, the friction coefficient increased with prolonged friction time. This figure also indicates that 1.5% MoS_2 nano-balls have advantages in terms of friction reduction over micro-MoS_2 and nano-slices within 30 min. The average friction coefficient of 1.5% MoS_2 nano-balls is 0.052, while those of 1.5% micro-MoS_2 and 1.0% nano-slices are 0.063 and 0.057, respectively. The differences among MoS_2 samples MoS_2 resulted from their different lubrication and wear mechanisms, which would be discussed in the following sections.

Figure 6 shows the variation of average WSD with increasing MoS_2 content. As shown in the figure, the influence of MoS_2 content on WSD was significantly correlated to the change in friction coefficients. LP samples with 1.5% MoS_2 nano-balls presented the lowest friction coefficients and the smallest WSDs. The difference between the antiwear properties of the nano-balls and nano-slices was not very notable; the samples with MoS_2 nano-slices also presented small WSDs. The tests confirm that nanosized MoS_2 has an advantage in terms of tribological properties over bulk 2H-MoS_2 under the selected conditions.

In summary, although the two nano-MoS_2 samples show observable advantages over micro-MoS_2, the differences between nano-ball and nano-slice are not very large under the selected testing conditions. The differences between the two nano samples were magnified at high rotation speeds in hydrodynamic lubrication region, and the application of nano-slices in high sliding speeds will be more advantageous. This would be discussed in the Sect. 3.5 concerning the lubrication mechanism using the Stribeck curves. Tribological results also indicate that the morphology of MoS_2 has an influence on the tribological properties of MoS_2. Adding the proper type of MoS_2 can improve the wear resistance and friction reduction of LP. Moreover,

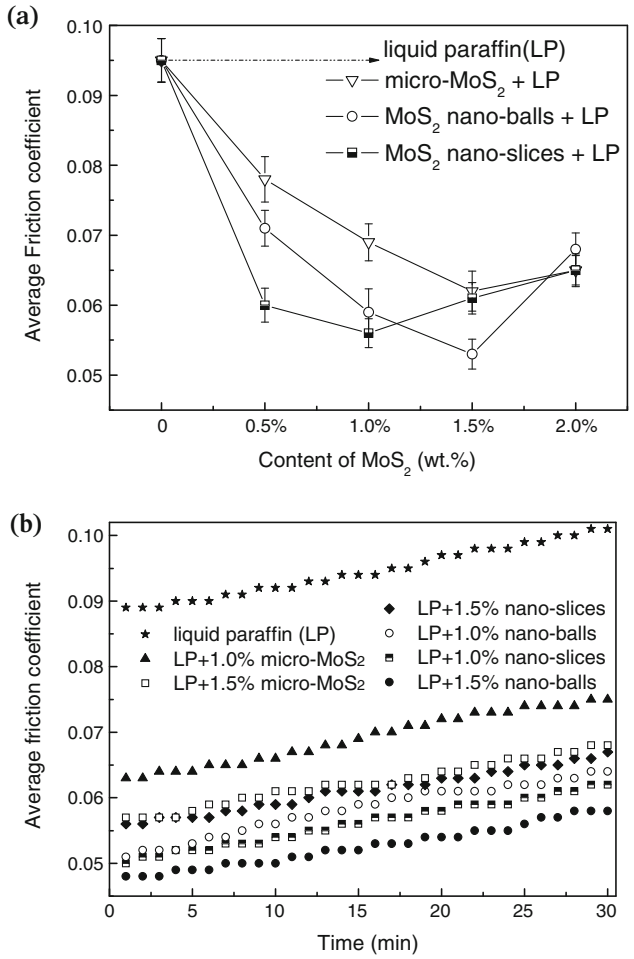

Fig. 5 Variation of average friction coefficients with: **a** increasing MoS_2 content in liquid paraffin and **b** increasing friction time (1,450 rpm and 300 N for 30 min)

considering the very simple preparation of nano-MoS_2, the benefit of adding nano-MoS_2 into LP is significant.

3.3 Micrographs of Wear Scars

Figure 7 provides the optical micrographs of typical wear scars on the bottom balls (1,450 rpm and 300 N for 30 min lubricated by LP with 1.5 wt% MoS_2). As shown in the figure, the WSDs of the bottom steel balls lubricated by nano-balls and nano-slices were smaller than those lubricated by micro-MoS_2. Differences between WSDs concerning the nano-balls and the nano-slices were not visible. The wear furrows from nano-MoS_2 were large and asymmetrically distributed on the wear area, while those lubricated by micro-MoS_2 homogenously appeared on the entire friction area. With high chemical activity, MoS_2 nanoparticles could easily enter the contact area of friction pairs to prevent steel balls from wear. Although nanoparticles have better anti-wear properties, they could easily agglomerate in the friction process and lead to inhomogeneous lubrication.

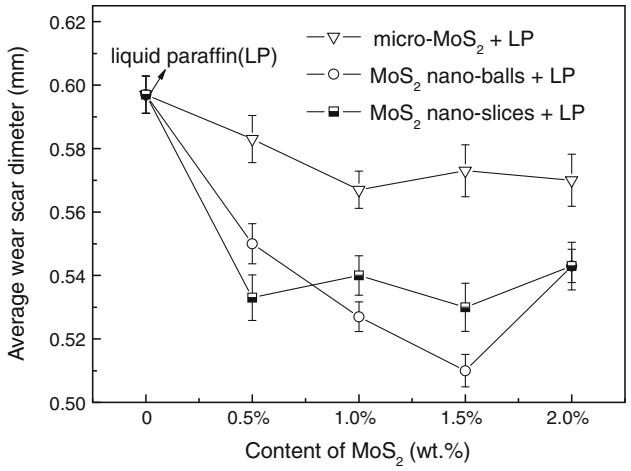

Fig. 6 Variation of the average wear scar with increasing MoS_2 content in liquid paraffin (1,450 rpm and 300 N for 30 min)

The figure also indicates that ploughing was the main manner of wear in the three bottom balls. Moreover, MoS_2 nano-slices with the highest chemical activities induced spalling wear on the contact area, which was responsible for the difference in the lubrication behavior of the nano-slices and the nano-balls at the content of 1.5 wt%. The chemical activities of MoS_2 in friction would be discussed using XPS results in the following section.

Figure 8 provides the optical micrographs of typical wear scars on the top balls (1,450 rpm and 300 N for 30 min lubricated by LP with 1.5 wt% MoS_2). As shown in the figure, the variation of wear scar widths on the top balls was almost consistent with that of the bottom balls. The top steel ball concerning nano-balls presented the smallest wear scar width, and the wear scar widths of the top steel balls lubricated by nano-balls and nano-slices were smaller than those lubricated by micro-MoS_2. The wear widths of the top balls varied from 0.8 to 1.0 mm, while the wear diameters of the bottom balls varied from 0.5 to 0.6 mm. The machining precision led to the observation that the three contact points did not locate at the same height. Thus, the wear width of the top ball was larger than the wear diameter of the bottom ball. Moreover, the figure confirms that ploughing was also the main manner of wear in the three top balls.

3.4 XPS Characterization of Wear Scars

Figure 9 shows the results of XPS analysis for the wear scars on the three top balls lubricated by LP with 1.5 wt% MoS_2 nano-balls, MoS_2 nano-slices, and micro-MoS_2, respectively, at 1,450 rpm under 300 N for 30 min. The peak at $\sim$232.8 eV (Fig. 9a) was caused by the Mo_{3d} of –Mo(VI)–O–, which results from the tribochemical reaction among MoS_2 nanoparticles, friction materials, and air.

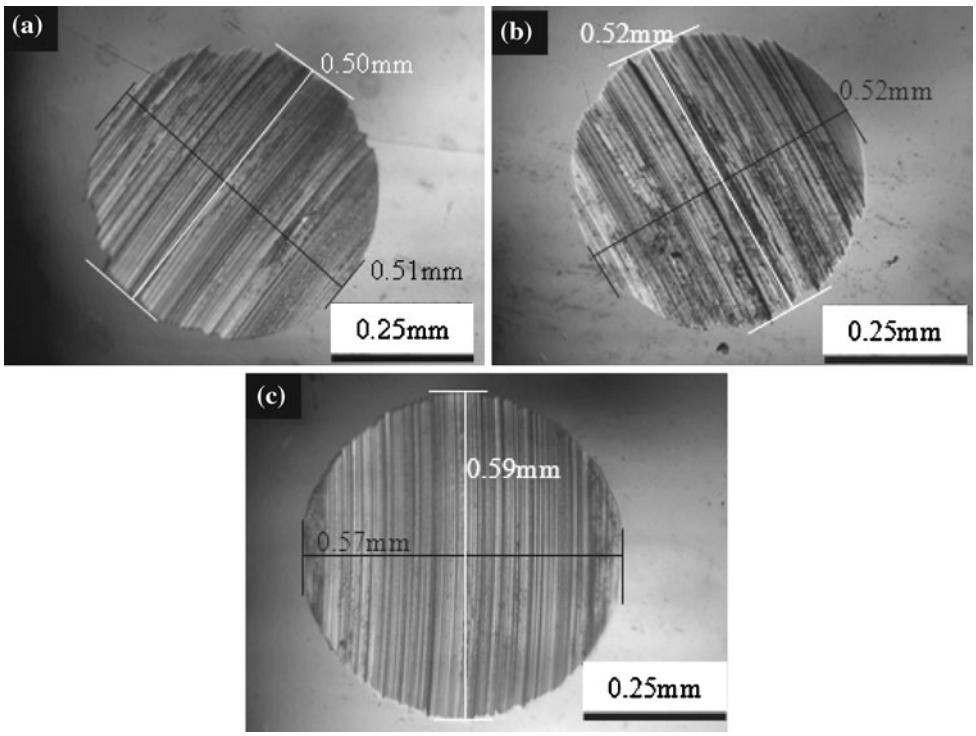

Fig. 7 Optical micrographs of typical wear scars on the bottom balls lubricated by LP with: **a** MoS_2 nano-balls, **b** MoS_2 nano-slices, and **c** micro-MoS_2 (1,450 rpm and 300 N for 30 min)

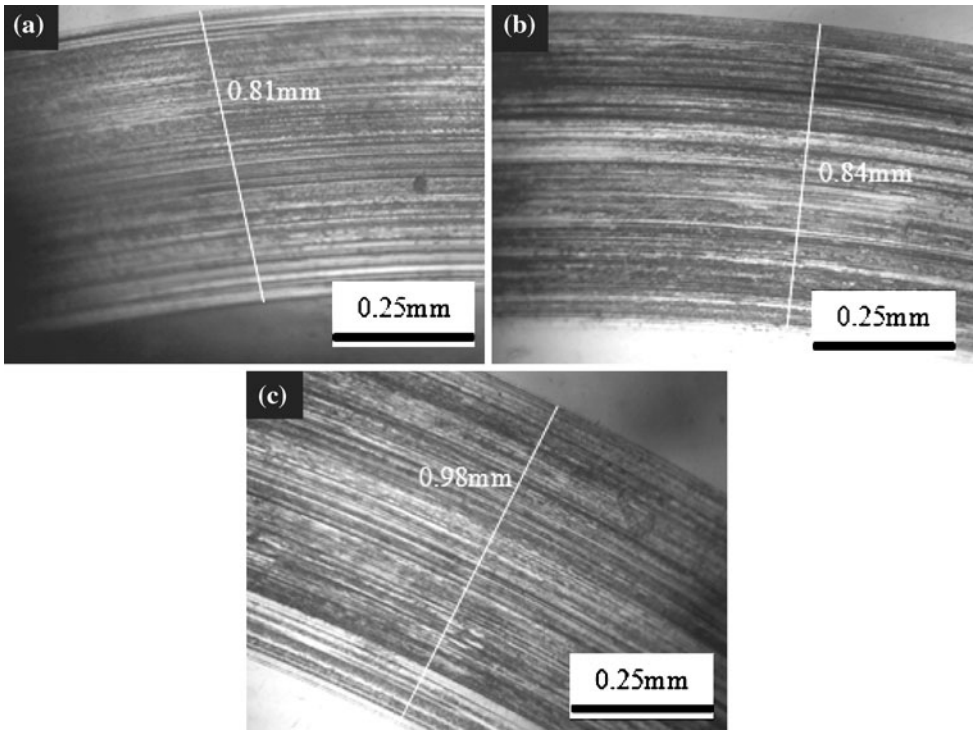

Fig. 8 Optical micrographs of typical wear scars on the top balls lubricated by LP with: (**a**) MoS_2 nano-balls, (**b**) MoS_2 nano-slices, and (**c**) micro-MoS_2 (1,450 rpm and 300 N for 30 min)

The peak at ~169.9 eV (Fig. 9b) was ascribed to the S_{2p} of –S(VI)–O–, the oxidation production of S. The peak at ~710.8 eV (Fig. 9c) is attributed to the Fe_{2p} of –Fe(III)–O–, which was produced by the tribological oxidization of steel. This was also confirmed by the O_{1s} peak at ~530.3 eV (Fig. 9d), which was caused by the O_{1s} of –Fe–O– and produced by the tribological oxidization of steel. Other O_{1s} peaks were induced by the tribological oxidization products of LP or contaminative –O–H, such as H_2O. The C_{1s} peak at ~285.2 eV (Fig. 9e) belongs to the –C–C– from LP or its oxidization products. However, the Mo_{3d} of MoS_2 was not found in the XPS spectra. The XPS characterization of the wear scar of the top ball was done after clearing the top ball in acetone using ultrasonic wave

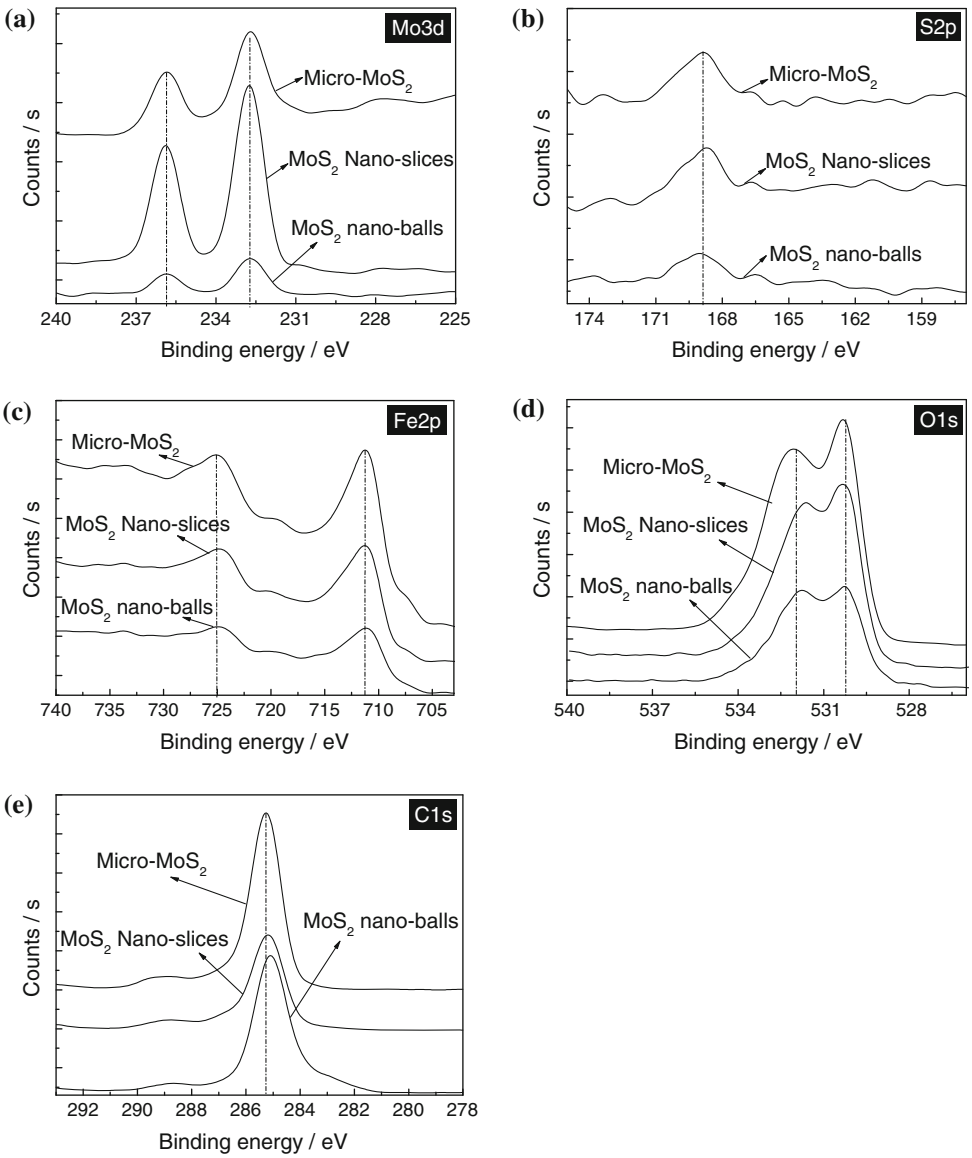

Fig. 9 XPS results of wear scars on the top balls lubricated by LP and MoS_2 at 1,450 rpm and 300 N for 30 min

and then drying at vacuum oven. The adsorbed substances such as MoS_2 were removed from the surface. Thus, the Mo_{3d} of –Mo–O– only was observed in the XPS spectra. These confirm that the oxidization film on the friction area of the steel ball is composed of MoO_3, Fe_2O_3, $Fe_2(SO_4)_3$, and carbon-containing compounds.

The XPS quantitative results in Table 1 reveal different oxidized extents between nano-MoS_2 and micro-MoS_2. As shown in the table, the quantity of Mo(VI) is 0.18 At% on the wear scars lubricated by MoS_2 nano-balls and 0.69 At% on the wear scars lubricated by MoS_2 nano-slices. This implies that MoS_2 nano-slices were oxidized more easily than nano-balls during the friction test, and that the chemical stability of nano-balls was higher than that of nano-slices. The oxidation extent of MoS_2 found in Ref. [21] is higher than that found in the present work. Tests in the reference were performed in a solid polyformaldehyde matrix under dry friction. In this work, however, they were performed in LP, which can rapidly transfer heat via convective heat transfer and decrease the effect of high temperatures on the oxidation of MoS_2 particles.

Generally, closed-structure MS_2 (M = Mo, W) without active dangling bonds is more difficult to oxidize than 2H-MS_2. Rapoport [13] reported that the oxidation temperature was about 350 °C for IF nanoparticles and 250 °C for 2H-WS_2 platelets (0.5 μm). The "rim-edge site" model of MoS_2 suggested that the layered structure of 2H-MoS_2 is composed of rim sites, edge sites, and basal surface [23]. The chemical activity of 2H-MoS_2 results from rim sites and edge sites, which have many chemical dangling bonds. However, the basal surface is not very active. The nano-slices used in this work have many highly active rim and

Table 1 XPS quantitative results of wear scars on the top balls lubricated by LP with 1.5 wt% MoS_2 at 1,450 rpm and 300 N for 30 min

Lubricants	LP + MoS_2 nano-balls		LP + MoS_2 nano-slices		LP + Micro-MoS_2	
	Peak/eV	At%	Peak/eV	At%	Peak/eV	At%
C1s	285.09	73.24	285.19	50.97	285.24	57.58
S2p	168.96	0.47	168.93	0.65	168.73	0.37
Mo3d	232.88	0.18	232.73	0.69	232.78	0.27
Fe2p	710.6	3.67	710.75	8.52	710.92	6.27
O1s Scan A	530.34	10.35	530.35	17.45	530.28	14.61
O1s Scan B	531.99	9.94	531.87	17.02	531.99	15.88
O1s Scan C	533.5	2.16	533.29	4.7	533.38	5.01

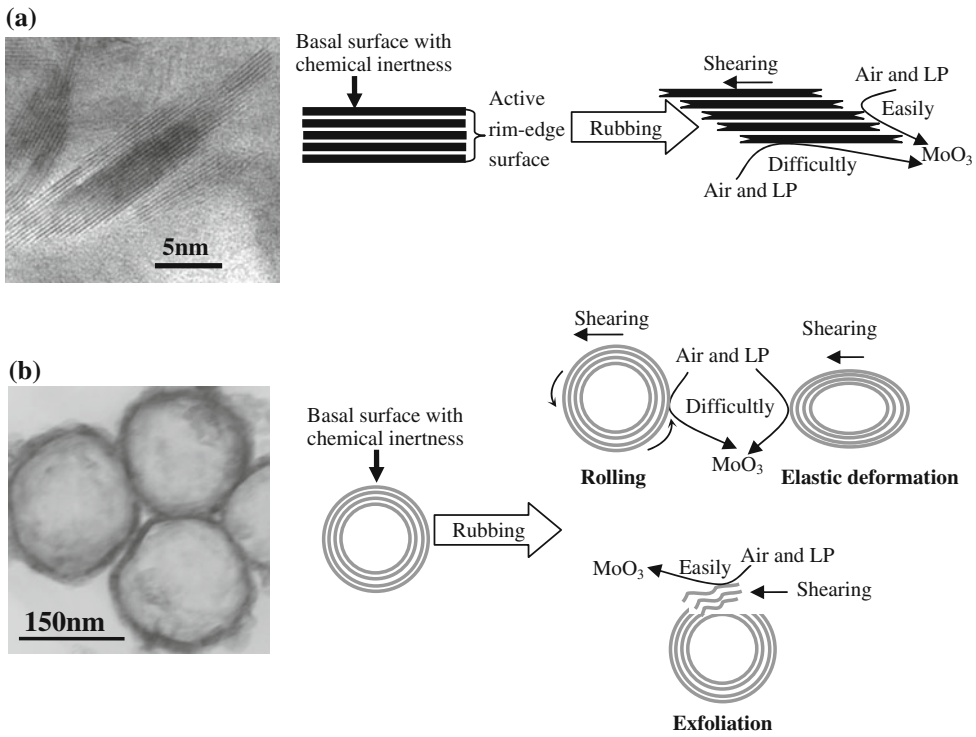

Fig. 10 Micrographs, schematic of nano-ball and nano-slice, and lubrication–wear mechanism of **a** MoS_2 nano-slices and **b** MoS_2 nano-balls

edge sites (Fig. 10a). Thus, nano-slices are easily oxidized into MoO_3 and weaken the lubrication effect in the friction process. The better tribological properties of nano-balls at the content of 1.5 wt% can be attributed to their chemical stability. Moreover, the excellent lubrication performances of spherical MoS_2 can be demonstrated by other mechanisms, such as rolling, elastic deformation, and exfoliation transferring [2, 13, 24].

Size is also an important factor that affects the chemical activity of MS_2 (M = Mo, W) particles. For example, the oxidation temperatures for IF nanoparticles and 2H-WS_2 platelets (4 μm) are about 350 and 420 °C, respectively [13]. The 2H-MoS_2, with sizes of ~30 μm, used in this work also have better chemical stability than nano-slices according to Table 1. However, the 2H-MoS_2 used presented worse tribological properties than nano-slices. The MoS_2 nano-slices have a higher Brunauer–Emmett–Teller (BET) surface area (41.8 m^2/g) than that of micro-MoS_2 (5.8 m^2/g) and MoS_2 nano-balls (19.5 m^2/g) [22]. The nano-slices show high chemical activity and easily enter into the contact area of the friction pair, thus functioning as a good lubricant.

The higher oxidation of nano-MoS_2 than micro-MoS_2 was also found in relative works reported by Wo and Wang et al. [3, 25]. The references proposed that oxidized products of MoS_2 such as MoO_3 can function as lubrication films. However, the oxidation of MoS_2 into MoO_3 (or "–Mo(VI)–O–") is generally considered as a reason for the invalidation of MoS_2 lubricant in friction processes because the oxidation destroys the lubrication structure of layered MoS_2. It was proposed in this work that a low oxidation has a positive effect on the lubrication, while a

too high oxidation presents a negative influence. Excessive oxidization was not found in the XPS results of the MoS_2 nano-slices (Mo 0.69%), which showed only approximately 2.5 times higher oxidization quantity than LP with $\sim$30 μm MoS_2 platelets (Mo 0.27%). Thus, MoS_2 nano-slices retained most of the advantages of nanoparticles, and presented better tribological properties than micro-MoS_2.

Moreover, the XPS data in Table 1 show a high carbon content on the surface lubricated by nano-balls. Among the chemicals used in this work, only liquid paraffin contained high carbon content. Thus, it was concluded that the high carbon content on the steel ball lubricated by nano-balls resulted from the easy friction reaction of LP on nano-balls. This can be explained by the curvature effect of the nano-ball. The 'rim-edge model' suggested that the active sites for catalytic reaction are located at the rim sites of MoS_2 [23], and at the basal surface there is no activity. The closed MoS_2 nano-ball only presented the curved basal surface without rim and edge sites which are considered as the active sites. However, the Ref. [26] reported that the MoS_2 nano-balls had an excellent catalytic activity in the degradation of organic chemicals. This indicates that the curved basal surface of the nano-ball is intrinsically different from the normal flat basal surface of the layered 2H-MoS_2. Curving slabs to form closed structure modified the structural properties of MoS_2 nano-balls, and the curvature effect of the nano-ball improved the catalytic performance for decomposing organic chemicals. The high carbon contamination on the friction surface resulted from the decomposing of liquid paraffin on the nano-balls during friction. The nano-slices also have a high activity in degrading organic chemicals such as methyl orange [26]. The different organic chemicals have different decomposing extents on the MoS_2 surface. Polyformaldehyde can decompose on the nano-slices, while it is stable on the nano-balls [21, 22]. Methyl orange can remarkably decompose on both nano-balls and nano-slices [26]. It was concluded that LP is easier to decompose on the nano-balls than nano-slices. This was also confirmed by the Stribeck curve of the nano-ball in LP, which would be discussed in the following section.

3.5 Lubrication Mechanism of MoS_2

The lubrication mechanism of layered 2H-MoS_2 is associated with the shearing of weak Van der Waals gaps between molecular layers. The structure of layer-opened MoS_2 nano-slices is similar to that of bulk 2H-MoS_2, thus also presenting shearing and sliding lubrication functions. The excellent tribological performance of fullerene-like nanoparticle is ascribed to its chemical inertness, rolling friction, deformation, exfoliation, and delivery of MoS_2 sheets to the contact area [2, 13, 24]. Due their spherical structure, MoS_2 nano-balls would have lubrication mechanisms similar to those of fullerene-like nanoparticles. The general lubrication and oxidation behaviors of nano-MoS_2 are demonstrated in Fig. 10.

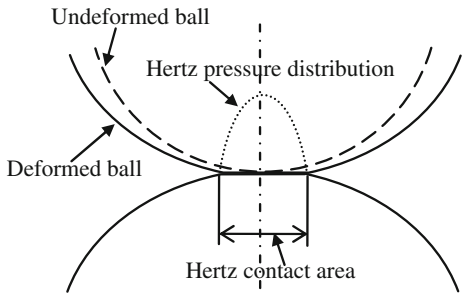

Fig. 11 Schematic of Hertz pressure distribution on the balls

However, the distance between the friction pair might be too small to permit effective rolling or even entry of MoS_2 to the contact area. The entry amounts of MoS_2 samples in the interface were different because of their different sizes. Thus, the XPS data did perhaps not reflect the actual oxidation degree of Mo. The lubrication mechanism mentioned above did not possibly work in the testing conditions used, which would be clarified by the Stribeck curves in the following discussion.

The tribological differences of MoS_2 samples used are demonstrated by their Stribeck curves. The Hertz pressure distribution at the point of contact in this work was demonstrated in Fig. 11, and the average pressure (p) may be calculated according to the formula:

$$p = F/\left(\pi a^2/4\right)$$

where a Hertz contact diameter, F load (300 N).

The contact diameter in the Hertz area (a) may be calculated via the following formula [27]:

$$a = 2\left(\frac{2}{3}\cdot\frac{FR}{E'}\right)^{\frac{1}{3}}$$

where R radius of steel ball (0.00635 m), E' elastic modulus (205 GPa), F load (300 N).

A constant load of 300 N was used in this work. Thus, the average pressure can be calculated as follows:

$$\begin{aligned} p &= F/\left[\pi\times\left(\frac{2}{3}\cdot\frac{FR}{E'}\right)^{\frac{2}{3}}\right] \\ &= 300/\left[3.14\times\left(\frac{2}{3}\times\frac{300\times 0.00635}{2.05\times 10^{11}}\right)^{\frac{2}{3}}\right] \\ &= 2.8\times 10^9\ \mathrm{N/m^2}. \end{aligned}$$

According to these mentioned above, the relationship of the Stribeck curve between the friction coefficient (μ) and $u\eta/p$ [u sliding speed; η viscosity of LP (0.015 Pa s at 25 °C)] can be obtained. The viscosity of LP varied with the increased temperature and prolonged friction time,

which is difficult to be measured in real time in this work. Thus, the result was calculated according to the average viscosity (η 0.012 Pa s) between the beginning and the end of the friction tests.

$$\frac{u\eta}{p} = \frac{u \times 0.012\,\text{Pa s}}{2.8 \times 10^9\,\text{N/m}^2} = 4.29 \times 10^{-12} u\ \text{m}.$$

The Stribeck curves of the LP with 1.0 wt% MoS_2 were obtained and shown in Fig. 12. This figure shows that the boundary lubrication occurred from 800 to 1,200 rpm, while the mixed lubrication from 1,200 to 1,500 rpm. The rotation speed used in this work (1,450 rpm) fell at the end of the mixed lubrication. The oil film thickness (h) and the distance between the friction pairs (the interface space) is very small ($h \rightarrow 0$) in the boundary lubrication region [28]. This indicates that the all MoS_2 nanoparticles should not enter the interface space, and that the all LP samples should show the same coefficients. However, the two MoS_2 nanoparticles presented better lubrication performances than the micro-MoS_2 in the boundary lubrication region (Fig. 12). This implies that few MoS_2 particles entered the interface even in the boundary lubrication region, which possibly resulted from the adsorption before loading. The nanoparticles with high BET surface areas [22] are easier to be adsorbed on the surface of steel balls, and showed better lubrication than micro-MoS_2.

In the mixed lubrication region, the oil film thickness is close to the surface roughness (R) of the friction pairs [28]. The balls used have a roughness of 0.032 μm (G20, GB/T308-2002 of China). Thus, the MoS_2 nano-slices easily penetrated the interface of the friction pairs and presented the lowest friction coefficient (Fig. 12). When the rotation speed was located at the hydrodynamic lubrication region, the oil film thickness increased, and more nano-balls could enter the interface. Consequently, the tribological difference between nano-balls and nano-slices was decreased at a rotation speed lower than 1,600 rpm. However, when the rotation speed was increased to 1,650 rpm, the friction of LP with nano-balls sharply increased, which was contradictory to the excellent lubrication performances of the spherical MoS_2 proposed by Chhowalla et al. [2, 13, 24]. According to the discussion mentioned above, it can be concluded that the curved basal surface of the nano-ball has high activity in decomposing LP, especially at high rotation speed which produces abundant rubbing heat. Accordingly, the tribological properties of nano-balls were influenced.

The increase in the content of nano-slices from 1.0 to 1.5 wt% enabled more nano-slices to enter the interface. However, due to the smaller sizes and easier penetration of the nano-slices, their amount in the interface had been enough to lubricate the steel balls at 1.0 wt%. Moreover, the space between the friction pairs was limited and could not contain so many nano-slices at 1.5 wt%. Thus, the increase from 1.0 to 1.5 wt% could not improve the lubrication effect of nano-slices (Fig. 5). However, the increase in the content of nano-balls to 1.5 wt% would induce more nano-balls into the interface. Because of the lubrication advantages of spherical MoS_2, the nano-balls showed a lower friction than nano-slices at 1.5 wt%. Moreover, a high content of MoS_2 increased the collision probability of MoS_2 particles which were dispersed by ultrasonic wave. The easy agglomerating of the dispersed MoS_2 led an increase in friction coefficient when the content was more than 1.0 wt% for nano-slices and 1.5% for nano-balls.

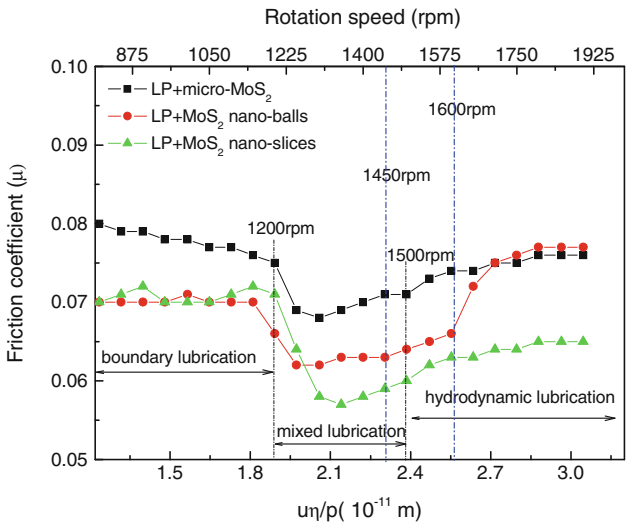

Fig. 12 Stribeck curves of steel balls lubricated by liquid paraffin and MoS_2 particles in point-contact friction

4 Conclusion

1. The tribological properties of liquid paraffin (LP) can be improved using MoS_2 additives, including nano-balls, nano-slices, and bulk 2H-MoS_2. Nanosized MoS_2 functions as a lubrication additive in LP better than bulk 2H-MoS_2.
2. The tribological properties of LP are influenced by the morphology and content of MoS_2 additives. Layer-closed MoS_2 nano-balls have a tribological advantage over MoS_2 nano-slices at 1.5 wt% content. The positive lubrication effect of MoS_2 nano-balls on LP is ascribed to the chemical stability of the closed layered structure.
3. The boundary lubrication occurs before 1,200 rpm under 300 N, while the mixed lubrication in 1,200–1,500 rpm. The 1,450 rpm used is located at the end of the mixed lubrication under 300 N. MoS_2 nano-slices have small sizes (5–10 nm in thickness)

and easily enter into the contact region of the friction pair with a roughness of 0.032 μm, functioning as lubrication additives in LP better than nano-balls do at the MoS_2 content of 1.0 wt%.

4. The Stribeck curves show that the lubrication properties of nano-slices were improved at high rotation speeds in hydrodynamic lubrication region. The application of nano-slices in high sliding speeds will be more advantageous.

Acknowledgments The authors wish to express their thanks to Mr. Y. Q. Zhou and Mr. X. Y. Wang for their assistance in the present work. This work was supported by the National Natural Science Foundation of China (Grant No. 50905054), the Anhui Provincial Foundation for Excellent Young Talents in University (Grant No. 2010SQRL160), and the Foundation of State Key Laboratory of Solid Lubrication (Grant No. 0907).

References

1. Hu, X.G., Hu, S.L., Zhao, Y.S.: Synthesis of nanometric molybdenum disulphide particles and evaluation of friction and wear properties. Lubr Sci. **17**, 295–308 (2005)
2. Chhowalla, M., Amaratunga, G.A.J.: Thin films of fullerene-like MoS_2 nanoparticles with ultra-low friction and wear. Nature **407**, 164–167 (2000)
3. Wo, H.Z., Hu, K.H., Hu, X.G.: Tribological properties of MoS_2 nanoparticles as additive in a machine oil. Tribology **24**, 33–37 (2004). (in Chinese)
4. Peng, Y.Y., Meng, Z.Y., Zhong, C., Lu, J., Yang, Z.P., Qian, Y.T.: Tube- and ball-like amorphous MoS_2 prepared by a solvothermal method. Mater. Chem. Phys. **73**, 327–329 (2002)
5. Zhan, J.H., Zhan, Z.D., Qian, X.F., Wang, C., Xie, Y., Qian, Y.T.: Solvothermal synthesis of nanocrystalline MoS_2 from MoO_3 and elemental sulfur. J. Solid State Chem. **141**, 270–273 (1998)
6. Li, W.J., Shi, E.W., Ko, J.M., Chen, Z.Z., Ogino, H., Fukuda, T.: Hydrothermal synthesis of MoS_2 nanowires. J. Cryst. Growth **250**, 418–422 (2003)
7. Nath, M., Govindaraj, A., Rao, C.N.R.: Simple synthesis of MoS_2 and WS_2 nanotubes. Adv. Mater. **13**, 283–286 (2001)
8. Zou, T.Z., Tu, J.P., Huang, H.D., Lai, D.M., Zhang, L.L., He, D.N.: Preparation and tribological properties of inorganic fullerene-like MoS_2. Adv. Eng. Mater. **8**, 289–293 (2006)
9. Afanasiev, P., Xia, G.F., Berhault, G., Jouguet, B., Lacroix, M.: Surfactant-assisted synthesis of highly dispersed molybdenum sulfide. Chem. Mater. **11**, 3216–3219 (1999)
10. Feldman, Y., Wasserman, E., Srolovitz, D.J., Tenne, R.: High rate, gas phase growth of MoS_2 nested inorganic fullerenes and nanotubes. Science **267**, 222–225 (1995)
11. Wilcoxon, J.P., Newcomer, P.P., Samara, G.A.: Synthesis and optical properties of MoS_2 and isomorphous nanoclusters in the quantum confinement regime. J. Appl. Phys. **81**, 7934–7944 (1997)
12. Huang, H.D., Tu, J.P., Zou, T.Z., Zhang, L.L., He, D.N.: Friction and wear properties of IF–MoS_2 as additive in paraffin oil. Tribol. Lett. **20**, 247–250 (2005)
13. Rapoport, L., Feldman, Y., Homyonfer, M., Cohen, H., Sloan, J., Hutchison, J.L., Tenne, R.: Inorganic fullerene-like material as additives to lubricants: structure–function relationship. Wear **225–229**, 975–982 (1999)
14. Cizaire, L., Vacher, B., Mogne, T.L., Martin, J.M., Rapoport, L., Margolin, A., Tenne, R.: Mechanisms of ultra-low friction by hollow inorganic fullerene-like MoS_2 nanoparticles. Surf. Coat. Technol. **160**, 282–287 (2002)
15. Rapoport, L., Fleischer, N., Tenne, R.: Applications of WS_2 (MoS_2) inorganic nanotubes and fullerene-like nanoparticles for solid lubrication and for structural nanocomposites. J. Mater. Chem. **15**, 1782–1788 (2005)
16. Hu, J.J., Bultman, J.E., Zabinski, J.S.: Inorganic fullerene-like nanoparticles produced by arc discharge in water with potential lubricating ability. Tribol. Lett. **17**, 543–546 (2004)
17. Rosentsveig, R., Gorodnev, A., Feuerstein, N., Friedman, H., Zak, A., Fleischer, N., Tannous, J., Dassenoy, F., Tenne, R.: Fullerene-like MoS_2 nanoparticles and their tribological behavior. Tribol. Lett. **36**, 175–182 (2009)
18. Rapoport, L., Nepomnyashchy, O., Verdyan, A., Popovitz-Biro, R., Volovik, Y., Ittah, B., Tenne, R.: Polymer nanocomposites with fullerene-like solid lubricant. Adv. Eng. Mater. **6**, 44–48 (2004)
19. Hu, K.H., Hu, X.G.: Formation, exfoliation and restacking of MoS_2 nanostructures. Mater. Sci. Technol. **25**, 407–414 (2009)
20. Hu, K.H., Wang, Y.R., Hu, X.G., Wo, H.Z.: Preparation and characterisation of ball-like MoS_2 nanoparticles. Mater. Sci. Technol. **23**, 242–246 (2007)
21. Hu, K.H., Wang, J., Schraube, S., Xu, Y.F., Hu, X.G., Stengler, R.: Tribological properties of MoS_2 nano-balls as filler in plastic layer of three-layer self-lubrication bearing materials. Wear **266**, 1198–1207 (2009)
22. Hu, K.H., Hu, X.G., Sun, X.J.: Morphological effect of MoS_2 nanoparticles on catalytic oxidation and vacuum lubrication. Appl. Surf. Sci. **256**, 2517–2523 (2010)
23. Daage, M., Chianelli, R.R.: Structure-function relations in molybdenum sulfide catalysts: the "rim-edge" model. J. Catal. **149**, 414–427 (1994)
24. Rapoport, L., Bilik, Y., Feldman, Y., Homyonfer, M., Cohen, S.R., Tenne, R.: Hollow nanoparticles of WS_2 as potential solid-state lubricants. Nature **387**, 791–793 (1997)
25. Wang, T.M., Shao, X., Wang, Q.H., Liu, W.M.: Preparation and tribological behavior of polyimide MoS_2 intercalation composite. Tribology **25**, 322–327 (2005). (in Chinese)
26. Hu, K.H., Hu, X.G., Xu, Y.F., Pan, X.Z.: The effect of morphology and size on the photocatalytic properties of MoS_2. React. Kinet. Mech. Catal. **100**, 153–163 (2010)
27. Wang, W.Z., Huang, P.: Study on the lubrication state of frictional pairs with different surface roughness based on Stribeck curves. Tribology **24**, 254–257 (2004). (in Chinese)
28. Li, H.Z., Zhang, X.H.: Study on the evaluation method of lubricating oils based on Stribeck curves. Lubr. Oil **24**, 61–64 (2009). (in Chinese)